ARTICLE

DNA-Functionalized Monolithic Hydrogels and Gold Nanoparticles for Colorimetric DNA Detection

Ajfan Baeissa, Neeshma Dave, Brendan D. Smith, and Juewen Liu*

Department of Chemistry, Waterloo Institute for Nanotechnology, University of Waterloo, 200 University Avenue West, Waterloo, Ontario N2L 3G1, Canada

ABSTRACT Highly sensitive and selective DNA detection plays a central role in many fields of research, and various assay platforms have been developed. Compared to homogeneous DNA detection, surface-immobilized probes allow washing steps and signal amplification to give higher sensitivity. Previously research was focused on developing glass or gold-based surfaces for DNA immobilization; we herein report hydrogel-immobilized DNA. Specifically, acrydite-modified DNA was covalently functionalized to the polyacrylamide hydrogel during gel formation. There are several advantages of these DNA-functionalized monolithic hydrogels. First, they can be easily handled in a way similar to that in homogeneous assays. Second, they have a low optical background where, in combination with DNA-functionalized gold nanoparticles, even ~0.1 nM target DNA can be visually detected. By using the attached gold nanoparticles to catalyze the reduction of Ag^+, as low as 1 pM target DNA can be detected. The gels can be regenerated by a simple thermal treatment, and the regenerated gels perform similarly to freshly prepared ones. The amount of gold nanoparticles adsorbed through DNA hybridization decreases with increasing gel percentage. Other parameters including the DNA concentration, DNA sequence, ionic strength of the solution, and temperature have also been systematically characterized in this study.

KEYWORDS: hydrogels • nanoparticles • DNA • colorimetric sensors • immobilization • gold

INTRODUCTION

Highly sensitive DNA detection plays a central role in many fields of research including genomics, disease diagnosis, bacterial and viral detection, forensic science, and bioanalytical chemistry (1−4). One of the standard methods for ultrasensitive DNA detection is the polymerase chain reaction (PCR), which usually requires a thermocycler in the molecular biology laboratory setting. This has led to an active pursuit in the development of other methods to minimize the use of sophisticated instrumentation. DNA detection can be achieved using either homogeneous assays or surface-immobilized probes. In the case of homogeneous assays, both sensor and target DNA are dissolved in the same solution and a signal is generated without a separation step. Such assays are preferred because of their simplicity. The sensitivity, however, is limited by the background signal because there are no separation steps and it is difficult for signal amplification to occur. On the other hand, rigorous washing steps can be performed for immobilized probes to minimize nonspecific binding, and signal amplification mechanisms can be introduced to achieve high sensitivity (5, 6). The operation, however, is more complex in comparison to homogeneous assays.

The majority of the early work for DNA detection employed fluorophores, enzymes, or radioisotopes as labels (7). While these labels allow highly sensitive DNA detection, specialized instruments or signal development steps are required. In the past 15 years, metallic nanoparticles have emerged as a new class of colorimetric labels for ultrasensitive bioassays (1, 3, 8−11). In comparison to organic dyes, metallic nanoparticles possess much higher extinction coefficients (e.g., 3−5 orders of magnitude higher than organic dyes), allowing visual detection at the nano- to picomolar concentrations (12). Similar to enzymes, metallic nanoparticles such as gold and platinum also possess catalytic activities, which can be used for signal amplification. Gold nanoparticles (AuNPs) are particularly attractive because thiol-modified DNA can be attached via the well-established thiol−gold chemistry.

There are several assay platforms designed for AuNP-based DNA detection, and homogeneous assays were developed first (1, 13, 14). In a typical system, two kinds of DNA-functionalized AuNPs were prepared with different DNA sequences so that the addition of the target DNA induces AuNP aggregation, which is accompanied by a red-to-purple color change due to surface plasmon coupling. Subnanomolar DNA can be detected using this method. However, the red-to-purple color change is not very sensitive to the human eye, especially at low target concentrations, making it necessary to perform a color enhancement step by spotting the solution on a white background, such as a thin-layer chromatography plate (1, 13). AuNP probes have also been used for immobilized DNA sensors (5, 15). In general, one DNA probe is immobilized on a glass surface and the other probe is attached to AuNPs. In the presence of the target DNA, the AuNPs are immobilized on the glass surface. The immobilized AuNPs can catalyze the reduction

* To whom correspondence should be addressed. E-mail: liujw@uwaterloo.ca.
Received for review August 23, 2010 and accepted November 3, 2010

DOI: 10.1021/am100780d

Published on Web 11/15/2010

of silver ions to metallic silver to enhance the optical density on the surface. With multiple amplification steps, a sensitivity similar to that of the PCR can be achieved (16).

While glass and gold surfaces are among those most frequently used for DNA immobilization, other surfaces such as paper (17−19), diamond (20), silicon (21), and lipid bilayer (22) have also been tested. We seek to engineer surfaces that allow convenient operation like in homogeneous assays, can be observed by the naked eye with a low optical background, and can still maintain the signal amplification capability of immobilized sensors. Hydrogels are cross-linked hydrophilic polymers that have attracted much recent research interest in many fields, including the making of sensors (23−28). Hydrogels are ideal for immobilization of biomolecules because the majority of their volume is water and biomolecules can maintain their native structure and function (29−32). A number of DNA-functionalized hydrogels have been reported for various applications (23−26, 33−41). Most of the work done on hydrogel-based sensors has focused on gel physical properties (e.g., swelling or phase transition) for making stimuli-responsive smart materials (42−44). Other signaling mechanisms such as electrochemical detection have also been demonstrated, while few examples of optical sensors are known (25, 30, 45−49). In particular, very few colorimetric sensors have been reported (25, 45, 50, 51). We are interested in making hydrogel-based colorimetric sensors because hydrogels are transparent and can therefore be observed with a low optical background, allowing a low concentration of labels to be visually detected. Herein, we demonstrate that highly sensitive colorimetric DNA detection can be prepared using DNA-functionalized monolithic hydrogels and AuNPs. The kinetics of color change, melting property, effect of the hydrogel percentage and DNA concentration, and hydrogel regeneration have been systematically studied.

EXPERIMENTAL SECTION

Chemicals. All of the DNA samples were purchased from Integrated DNA Technologies (Coralville, IA). See Table 1 for DNA sequences and modifications. A 29:1 gel stock solution of 40% acrylamide/bisacrylamide, ammonium persulfate (APS), and *N*,*N*,*N*′,*N*′-tetramethylethylenediamine (TEMED) were purchased from VWR (Mississauga, Ontario, Canada). Sodium dodecyl sulfate (SDS), $NaNO_3$, NaCl, tris(hydroxymethyl)aminomethane (Tris), and 4-(2-hydroxyethyl)-1-piperazineethanesulfonic acid (HEPES) were purchased from Mandel Scientific (Guelph, Ontario, Canada). SYBR Green I (10 000×) in dimethyl sulfoxide (DMSO) was purchased from Invitrogen (Carlsbad, CA). Colloidal AuNPs (50 nm) were purchased from Ted Pella (Redding, CA). The silver enhancement kit and tris(2-carboxyethyl)phosphine (TCEP) were purchased from Sigma-Aldrich. For most of the experiments, Tris nitrate at pH 8.0 was used to maintain the pH. Millipore water was used for all of the experiments.

Preparation of DNA-Functionalized Hydrogels. Monolithic polyacrylamide hydrogels were prepared by mixing the following solutions: 40% gel stock solution (29:1), $NaNO_3$ (2 M), Tris nitrate (pH 8.0, 0.5 M), acrydite DNA (0.5 mM), and water. This solution contained a final gel percentage of 4%, 100 mM $NaNO_3$, 50 mM Tris nitrate, and 10 μM DNA. To initiate polymerization, an initiator solution was added. The initiator solution was immediately used after the preparation by dissolving 50 mg of APS in 500 μL of water, to which 25 μL of TEMED was added (24, 35). In the final solution, the volume of the initiator was kept at 5%. A 96-well plate was used to prepare the gel, and to each well was added 75 μL of the gel solution. After 1 h of polymerization at room temperature, the formed hydrogels were washed three times by soaking the gels in 100 mM NaCl, 20 mM HEPES, pH 7.6 (at least 3 h for each soaking). The purpose of this was to remove unreacted monomers, initiators, and free DNA. Subsequent to soaking, each gel was transferred to a 1.5 mL microcentrifuge tube and was ready for use. For some experiments, different gel percentages were used. To quantify the DNA conjugation efficiency, a SYBR Green I based assay was used, as described in the literature (28).

Table 1. Different DNA Sequences and Modifications Used in This Work[a]

name	sequences and modifications (listed from 5′ to 3′)
acrydite DNA	Acrydite-CTTCTTTCTTCCCCTTGTTTGTTG
thiol DNA	TCACAGATGCGTAAAAAAAAA-SH
FAM DNA	FAM-CACTGACCTGGG
target DNA	TTTACGCATCTGTGACAACAAACAAGGGGA
G · T mismatch	TTTACG<u>T</u>ATCTGTGACAACAAACAAGGGGA
G · A mismatch	TTTACG<u>A</u>ATCTGTGACAACAAACAAGGGGA
G · G mismatch	TTTACG<u>G</u>ATCTGTGACAACAAACAAGGGGA
FAM linker	CCCAGGTCAGTGCAACAAACAAGGGGA
c-acrydite DNA	CAACAAACAAGGGGAAGAAAGAAG

[a] The mutated nucleotides in the mismatched DNAs are highlighted by an underline.

Preparation of DNA-Functionalized AuNPs. AuNPs of 13 nm were prepared and functionalized as described in the literature (13). AuNPs of 50 nm were functionalized following protocols described in the literature with slight modifications (52). The thiol-modified DNA was first activated with a 1-fold excess of TCEP for 1 h at room temperature. The 50 nm AuNPs were mixed with 1 μM activated thiol DNA for 1 h in the presence of 0.01% SDS. The sample was brought to 5 mM HEPES, pH 7.6, with 50 mM NaCl and incubated for another 1 h. The sample was then sonicated for 10 s, and to this was added another portion of 50 mM NaCl. After overnight incubation, the AuNPs were ready for use and can survive the 300 mM NaCl required for our experiment.

DNA Detection and Silver Enhancement. For DNA detection, each gel was soaked in 1 mL of buffer containing 1.2 nM 13 nm AuNPs and varying concentrations of the target DNA in 300 mM NaCl, 20 mM HEPES, pH 7.6. After 2 h at room temperature, the supernatant was removed and the gels were resuspended in the same buffer and imaged. Because of the self-aggregation tendency of 50 nm AuNPs (53), detection with 50 nm AuNPs was carried out at 50 °C. For silver enhancement, solutions A and B from the kit were mixed 1:1 right before use. Each gel after AuNP binding was soaked in buffer (50 mM $NaNO_3$, 10 mM Tris nitrate, pH 8.0) three times at 4 °C to remove free AuNPs and Cl^-. The gels were then each mixed with 1 mL of the mixed silver enhancement solution and were soaked in the dark for 1 h at room temperature.

Melting Curves and Kinetics. To measure melting curves, a gel (75 μL) with immobilized AuNPs was soaked in a buffer (20 mM NaCl, 10 mM HEPES, pH 7.6) twice for 1 h at 4 °C and placed in a quartz microcuvette containing 400 μL of the same buffer. The gel sizes are large enough to sit on top of the optical window for detection but still small enough to move freely in the buffer. The cuvette was sealed on the top by parafilm to prevent evaporation. Extinction at 520 nm was then monitored as a function of the temperature using an Agilent 8453 spectrophotometer. The temperature was increased at a rate of 1 °C/min. The sample was equilibrated for 3 min at each temperature before the measurement was taken. To monitor free

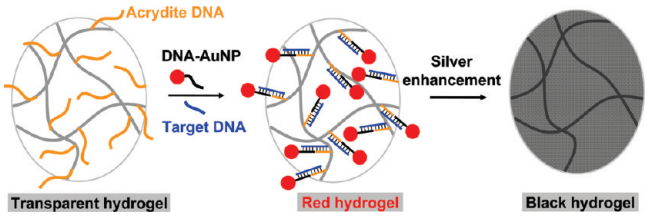

FIGURE 1. Schematic presentation of using DNA-functionalized hydrogels and AuNPs for colorimetric DNA detection. Transparent gels change color to red in the presence of the target DNA. Signal amplification can be achieved by reducing Ag^+ in the presence of AuNPs to coat the gel with metallic silver.

DNA melting, the involved DNAs were annealed at a concentration of 1 μM in the same buffer in 400 μL. The samples were run side-by-side to minimize systematic errors. For kinetic measurements, the gels were soaked in buffers containing varying concentrations of NaCl in the presence of 1.2 nM, 13 nm AuNP and 10 nM linker DNA and the decrease of the solution-phase AuNP extinction was monitored as a function of time.

FAM DNA Immobilization. FAM DNA and FAM linker (200 nM) were incubated with each gel in 1 mL of buffer containing 300 mM NaCl, 20 mM HEPES, pH 7.6. After 1 h, the gels were washed and dispersed in the same buffer and were imaged by excitation at 245 nm with a hand-held UV lamp.

Hydrogel Regeneration. After adsorption of AuNPs or the FAM DNA to the hydrogel surface, the hydrogels were regenerated by washing the gels twice in a buffer containing 5 mM HEPES at 50 °C for 10 min. After washing, the gels have lost most of the AuNPs or FAM-labeled DNA. The regenerated gels were then tested for adsorption of AuNPs or the FAM DNA in the presence of linker DNA using the protocol described above.

RESULTS AND DISCUSSION

Design of Hydrogel-Based Colorimetric DNA Sensors. The colorimetric sensor is constructed as shown in Figure 1. There are two kinds of probe DNA molecules. One is modified with an acrydite on the 5′ end to achieve covalent attachment to the polyacrylamide hydrogel matrix. The gel was prepared by mixing acrylamide, bisacrylamide, acrydite-modified DNA, and an initiator in a total volume of 75 μL. After 1 h of incubation at room temperature, the gel was formed with the DNA covalently attached to the gel. Nonincorporated DNA, free monomers, and initiators were removed by soaking the gels in a buffer. The other DNA contained a 3′-thiol modification for attachment to AuNPs. In the presence of the target DNA, the AuNPs are linked to the hydrogel surface to produce a red color on the gel surface. Because of their very high extinction coefficient, AuNPs can offer high sensitivity for visual detection. The sensitivity can be further increased by using the AuNPs as a catalyst for the reduction of silver ions to metallic silver to give a black color.

Effect of the Acrydite DNA Concentration. Because the acrydite DNA was attached to the hydrogel during its formation, DNA molecules are present not only on the gel surface but also inside the gel. To identify the optimal DNA concentration, eight gels formed in the presence of 0−10 μM acrydite DNA were prepared. The gels were incubated with 1.2 nM of 13 nm AuNPs and 10 nM target DNA for 2 h at room temperature. After the reaction, the

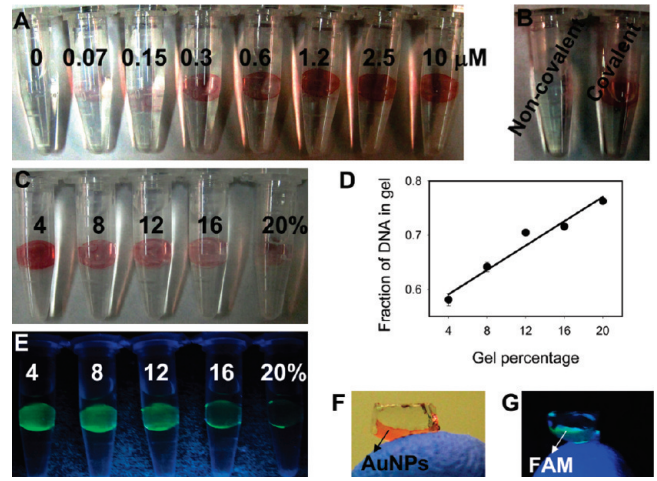

FIGURE 2. (A) DNA detection using hydrogels prepared with varying acrydite DNA concentrations. A higher DNA concentration gives higher color intensity. (B) Test of the importance of a covalent DNA linkage in the hydrogel. Without the acrydite group, no AuNP is immobilized and the gel cannot detect DNA. (C) Effect of the hydrogel percentage. All of the gels were prepared with 10 μM DNA. (D) Fraction of acrydite DNA incorporated in various percentage gels. Higher percentage gels contained more DNA. (E) Effect of the hydrogel percentage on immobilization of a FAM-labeled DNA through a linker DNA. (F and G) Photographs of 4% gels in parts C and E, respectively, after cutting with a razor blade. Only one of the surfaces has the AuNP or FAM label. The picture in part G was taken under 254 nm UV excitation. This result shows that only AuNPs or FAM DNA on the gel surface contributes to the observed optical signals.

color in the supernatant solution was still quite red for all of the samples, suggesting that AuNPs were in excess and the limiting factor should be the acrydite DNA density on the hydrogel surface. As shown in Figure 2A, the color progressively increased with increasing DNA concentration. If the acrydite DNA concentration was lower than 0.3 μM, barely any red color could be observed on the gels. In the absence of the acrydite DNA, there was almost no optical background, allowing a very small amount of AuNPs to be observed. This suggests that the nonspecific binding between the hydrogel and AuNP was very low. With >2.5 μM DNA, the gel showed a saturated intense red color. Therefore, we chose to use 10 μM DNA for subsequent experiments to ensure that there was sufficient DNA on the hydrogel surface. If the gel was prepared with the same DNA sequence but without acrydite modification, no AuNPs associated with the gel surface (Figure 2B). This is attributed to the lost DNA during the gel soaking in a buffer, suggesting that a covalent linkage is extremely important for the function of the gel.

Effect of the Hydrogel Percentage. Next the effect of the hydrogel percentage on AuNP immobilization was tested. With a higher gel percentage, the gel becomes harder and more brittle, while very low percentage gels (e.g., <3%) are very soft and difficult to handle. Therefore, polyacrylamide gels in the range of 4−20% have been prepared and incubated with AuNPs and target DNA. As shown in Figure 2C, the highest color intensity was observed with the 4% hydrogel and the color progressively decreased with higher gel percentages. The same trend was observed if the AuNP

probe was replaced by a FAM-labeled DNA (Figure 2E). Under UV excitation, the lower percentage gels also showed a much brighter fluorescence. The AuNPs (13 nm diameter) are much larger compared to the fluorophore label and can form multivalent linkages on the gel surface. The fact that these two probes showed a similar gel-percentage-dependent adsorption suggests that the inhibition of adsorption for high percentage gels is independent of the label. These experiments suggest that either fewer DNAs were incorporated in higher percentage gels or there was a lower density of DNA on the surface of higher percentage gels.

To test the main contributing factor, the acrydite DNA concentrations in the gels were quantified. The freshly prepared gels were soaked in a buffer for 1 day, and the soaking solutions were mixed with the cDNA of the acrydite DNA and SYBR Green I. SYBR Green I is fluorescent only in the presence of double-stranded DNA to give a green fluorescence. As shown in Figure 2D, a linear relationship was obtained from this experiment and more acrydite DNA was incorporated into higher percentage gels. For example, close to 60% DNA was attached to the 4% gel while ~80% DNA was in the 20% gel. Therefore, the lower AuNP or fluorescence intensity cannot be explained by the amount of DNA attached to the hydrogels.

To test whether the nanoparticle or fluorescent probes can penetrate into the interior of the gels, 4% gels were reacted with the AuNP or fluorophore probes and then cut with a razor blade such that only one surface was the original surface. From the images shown in Figure 2F,G, no AuNP or fluorophore can be detected by visual inspection in the interior of the gels and most of the color was on the surface. Taken together, the higher AuNP or fluorophore density in lower percentage gels should be attributed to the higher availability of surface DNA. Higher percentage gels have a smaller pore size and therefore smaller surface area, which may decrease the number of DNA units on the surface and contribute to the observations. Therefore, we chose to use 4% gels for subsequent experiments.

Hybridization Kinetics. DNA hybridization is strongly dependent upon the salt concentration. For DNA hybridization in solution, a higher salt generally offers faster hybridization kinetics. To study the DNA binding kinetics on the hydrogel surface, we have soaked gels in a solution containing DNA-functionalized AuNPs and target DNA at three different NaCl concentrations (10, 300, and 500 mM). The binding kinetics was monitored by the decrease of AuNP extinction at 520 nm in the solution phase. With a low salt concentration, the binding of AuNPs to the gel surface was very slow (Figure 3, black curve). Increasing the salt concentration to 300 mM increased the binding kinetics and about one-third of the AuNPs adsorbed onto the gel surface in 2 h. A further increase of NaCl to 500 mM did not significantly improve the kinetics. Therefore, 300 mM NaCl was chosen for subsequent experiments.

Melting Curve. One of the important tools to characterize DNA and DNA-linked nanoparticles is melting studies where, as the temperature increases, double-stranded DNA

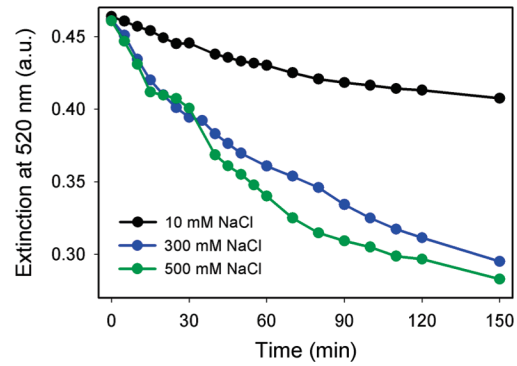

FIGURE 3. Kinetics of AuNP adsorption on the hydrogel surface at different salt concentrations.

dissociates and disrupts DNA linkages. In general, melting transitions are sharper in DNA-assembled nanostructures because of multivalent and cooperative DNA binding (12, 54). As shown in Figure 4A, the gels with immobilized AuNPs were soaked in temperature-controlled quartz microcuvettes. Initially, there was no extinction from the buffer. As the temperature was increased, AuNPs started to dissociate from the gel surface and the buffer became red. Some of the temperature-dependent extinction spectra are shown in Figure 4B, and the sharpest transition is observed around 44 °C. The melting curve was obtained by plotting the 520 nm extinction as a function of the temperature (Figure 4C, blue curve). For comparison, the same DNA sequences without AuNPs or gel were also melted under identical conditions (red curve). We performed this analysis by monitoring the hyperchromic effect of DNA at 260 nm. Indeed, the melting transition is broader compared to the AuNP–gel system (12), although these two systems showed identical melting temperatures (T_m). This experiment confirms that AuNPs were indeed linked to the gel surface through reversible DNA linkages, and gel surfaces were similar to other solid surfaces in terms of DNA melting properties (12). The relatively sharp melting transitions in our system may allow detection of DNA targets containing mismatches.

Sensitivity and Selectivity. With an understanding of the gel and AuNP properties, we next tested the sensitivity and selectivity of the gel for DNA detection. The 4% gels were soaked in 1 mL of buffer containing 1.2 nM AuNPs and varying concentrations of the target DNA. After 2 h, buffer was removed and the gels were soaked in new buffers without AuNPs. The gels were then imaged using a digital camera. As shown in Figure 5A, a slight red color can be observed with 0.1 nM target DNA and higher than 1 nM DNA generated an intense red color. This sensitivity is similar to those reported with other surfaces without signal amplification steps (5, 55). To improve the sensitivity, we first tested larger AuNPs. Compared to 13 nm AuNPs, 50 nm ones have an extinction coefficient of more than 2 orders of magnitude higher (12, 52, 56). Therefore, for the same number of adsorbed AuNPs, larger ones should give higher color intensity.

Under experimental conditions (300 mM NaCl), we noticed that 50 nm AuNPs self-aggregated at room temperature

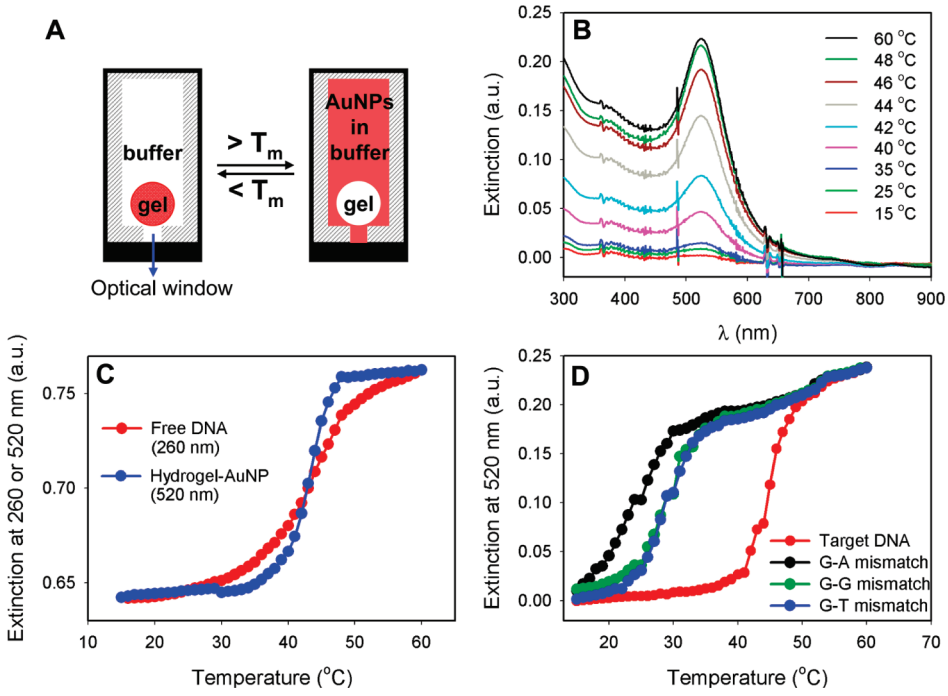

FIGURE 4. (A) Experimental setup for measuring hydrogel DNA melting curves. The gel with immobilized AuNPs was immersed in the buffer. Upon melting, AuNPs dissociate from the gel and are detected by an increase in the extinction of the buffer. (B) Selected spectra at several temperatures. (C) Melting curves of free DNA (monitored at 260 nm) and a hydrogel/AuNP conjugate (monitored at 520 nm). The curves were normalized for comparison of the transition sharpness and T_m. (D) Melting curves of a hydrogel/AuNP conjugate containing mismatched DNA targets.

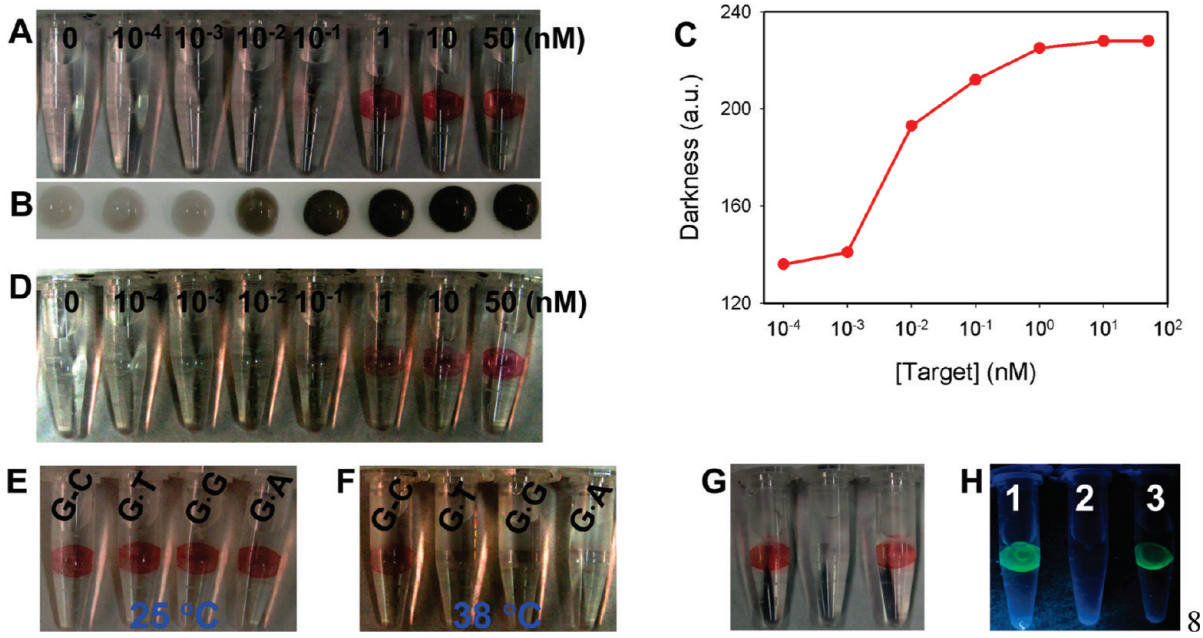

FIGURE 5. Sensitivity of DNA detection with 13 nm AuNPs (A) and after silver enhancement (B) and with 50 nm AuNPs (D). (C) Quantification of darkness in part B. Selectivity test with perfectly matched target DNA and DNA targets containing single base mismatches at 25 °C (E) and 38 °C (F). Test of hydrogel sensor regeneration with AuNPs (G) and FAM-labeled DNA (H). In parts G and H, the tubes marked 1−3 contained freshly prepared gels, gels after the regeneration treatment, and regenerated gels reacted with AuNPs or FAM-labeled DNA, respectively.

to change color to blue. Upon heating of the sample to 50 °C, the AuNPs disassembled to give a red color. Therefore, we chose to link the 50 nm AuNPs to hydrogel at 50 °C to eliminate the self-aggregation of heavily DNA-functionalized large AuNPs (53). T_m of the AuNP/gel hybrid was much higher than 50 °C, and this hybrid can still form. As shown in Figure 5D, a similar color response was observed. For the same linker DNA concentration, however, the 50 nm AuNPs were even less intense compared to the 13 nm ones. Because the extinction coefficient of 50 nm AuNPs is about 2 orders of magnitude higher than that of the 13 nm ones, this experiment suggests that the adsorbed 50 nm AuNPs were 2 orders of magnitude lower in number. The difference may be explained by the pore size of the hydrogel. For example, it is likely that our hydrogel has a pore size between 13 and 50 nm.

Because using larger AuNPs produced limited improvement on sensitivity, we next tested the use of immobilized AuNPs to catalyze the growth of silver. The gels were soaked using a commercial silver enhancement kit. After 1 h, the gels were taken out of the soaking solutions and imaged by a digital camera. As shown in Figure 5B, 13 nm AuNPs were able to catalyze the silver reduction reaction, and as quantified in Figure 5C, ~1 pM DNA can be detected, and this sensitivity is also comparable to the other surfaces after similar silver treatment steps (5, 55).

To test the selectivity of the gel-based detection system, target DNA molecules containing single base mismatches were used to immobilize AuNPs. All of the samples showed a similar red color at 25 °C (Figure 5E), suggesting that the mismatched DNAs were also quite stable in forming the linkages. The melting curves of these materials are shown in Figure 4D, and the matched DNA has a T_m of at least 15 °C higher compared to those of mismatched ones. Therefore, by warming of the gels to 38 °C, AuNPs linked by mismatched DNA were dissociated while the perfectly matched target was still capable of maintaining the AuNPs (Figure 5F).

Regeneration is one of the advantages of immobilized sensors. Because the AuNPs are attached to the gel via DNA linkages, regeneration can be achieved using a simple thermal denaturation step. To test this, the gel with AuNPs attached (Figure 5G, gel 1) was heated in a low ionic strength buffer (5 mM HEPES, pH 7.6) at 50 °C for 10 min. The majority of the AuNPs were released from the gel surface and the gel appeared to be transparent (Figure 5G, gel 2). When this regenerated gel was used, a color similar to that of the freshly prepared gel (Figure 5G, gel 3) was observed. The same trend was also observed when the FAM DNA was used (Figure 5H). These experiments suggest that the DNA density on the gel surface did not change after regeneration and the hydrogels can be easily regenerated.

CONCLUSIONS

In summary, we have demonstrated that monolithic hydrogels can be used as a surface for DNA immobilization with a very low optical background. A very low concentration of target DNA can be visually detected with DNA-functionalized AuNP probes. Compared to other commonly used surfaces for DNA immobilization, hydrogels can be molded into arbitrary shapes and handled in a way similar to that of homogeneous assays while still allowing washing and signal amplification to increase the sensitivity. A major advantage of hydrogels is the high capacity of AuNP adsorption, allowing convenient visual detection without the aid of any analytical instrument. At the same time, the hydrogel can be regenerated by a simple heat treatment. As demonstrated in this work, hydrogel-based surfaces have similar sensitivity compared to glass surfaces for DNA detection. The ability for the gel surface to adsorb AuNPs is affected by the gel percentage, DNA concentration, salt, and temperature. All of these parameters have been systematically characterized in this study.

Acknowledgment. Funding for this work is from the University of Waterloo and the Discovery Grant of the Natural Sciences and Engineering Research Council of Canada. A.B. received a scholarship from the Ministry of Higher Education of Saudi Arabia.

REFERENCES AND NOTES

(1) Elghanian, R.; Storhoff, J. J.; Mucic, R. C.; Letsinger, R. L.; Mirkin, C. A. *Science* **1997**, *277*, 1078–1080.
(2) Tan, W. H.; Wang, K. M.; Drake, T. J. *Curr. Opin. Chem. Biol.* **2004**, *8*, 547–553.
(3) Rosi, N. L.; Mirkin, C. A. *Chem. Rev.* **2005**, *105*, 1547–1562.
(4) Ho, H. A.; Najari, A.; Leclerc, M. *Acc. Chem. Res.* **2008**, *41*, 168–178.
(5) Taton, T. A.; Mirkin, C. A.; Letsinger, R. L. *Science* **2000**, *289*, 1757–1760.
(6) Yershov, G.; Barsky, V.; Belgovskiy, A.; Kirillov, E.; Kreindlin, E.; Ivanov, I.; Parinov, S.; Guschin, D.; Drobishev, A.; Dubiley, S.; et al. *Proc. Natl. Acad. Sci. U.S.A.* **1996**, *93*, 4913–4918.
(7) Wetmur, J. G. *Crit. Rev. Biochem. Mol. Biol.* **1991**, *26*, 227–259.
(8) Liu, J.; Cao, Z.; Lu, Y. *Chem. Rev.* **2009**, *109*, 1948–1998.
(9) Zhao, W.; Brook, M. A.; Li, Y. *ChemBioChem* **2008**, *9*, 2363–2371.
(10) Katz, E.; Willner, I. *Angew. Chem., Int. Ed.* **2004**, *43*, 6042–6108.
(11) Penn, S. G.; He, L.; Natan, M. J. *Curr. Opin. Chem. Biol.* **2003**, *7*, 609–615.
(12) Jin, R.; Wu, G.; Li, Z.; Mirkin, C. A.; Schatz, G. C. *J. Am. Chem. Soc.* **2003**, *125*, 1643–1654.
(13) Storhoff, J. J.; Elghanian, R.; Mucic, R. C.; Mirkin, C. A.; Letsinger, R. L. *J. Am. Chem. Soc.* **1998**, *120*, 1959–1964.
(14) Reynolds, R. A., III; Mirkin, C. A.; Letsinger, R. L. *J. Am. Chem. Soc.* **2000**, *122*, 3795–3796.
(15) Storhoff, J. J.; Lucas, A. D.; Garimella, V.; Bao, Y. P.; Muller, U. R. *Nat. Biotechnol.* **2004**, *22*, 883–887.
(16) Nam, J.-M.; Stoeva, S. I.; Mirkin, C. A. *J. Am. Chem. Soc.* **2004**, *126*, 5932–5933.
(17) Ali, M. M.; Aguirre, S. D.; Xu, Y. Q.; Filipe, C. D. M.; Pelton, R.; Li, Y. F. *Chem. Commun.* **2009**, 6640–6642.
(18) Zhao, W. A.; Ali, M. M.; Aguirre, S. D.; Brook, M. A.; Li, Y. F. *Anal. Chem.* **2008**, *80*, 8431–8437.
(19) Su, S. X.; Ali, M.; Filipe, C. D. M.; Li, Y. F.; Pelton, R. *Biomacromolecules* **2008**, *9*, 935–941.
(20) Ushizawa, K.; Sato, Y.; Mitsumori, T.; Machinami, T.; Ueda, T.; Ando, T. *Chem. Phys. Lett.* **2002**, *351*, 105–108.
(21) Bocking, T.; Killan, K. A.; Gaus, K.; Gooding, J. J. *Langmuir* **2006**, *22*, 3494–3496.
(22) Yoshina-Ishii, C.; Miller, G. P.; Kraft, M. L.; Kool, E. T.; Boxer, S. G. *J. Am. Chem. Soc.* **2005**, *127*, 1356–1357.
(23) Murakami, Y.; Maeda, M. *Macromolecules* **2005**, *38*, 1535–1537.
(24) Yang, H. H.; Liu, H. P.; Kang, H. Z.; Tan, W. H. *J. Am. Chem. Soc.* **2008**, *130*, 6320–6321.
(25) Zhu, Z.; Wu, C. C.; Liu, H. P.; Zou, Y.; Zhang, X. L.; Kang, H. Z.; Yang, C. J.; Tan, W. H. *Angew. Chem., Int. Ed.* **2010**, *49*, 1052–1056.
(26) Soontornworajit, B.; Zhou, J.; Shaw, M. T.; Fan, T. H.; Wang, Y. *Chem. Commun.* **2010**, *46*, 1857–1859.
(27) Tsitsilianis, C. *Soft Matter* **2010**, *6*, 2372–2388.
(28) Dave, N.; Huang, P.-J. J.; Chan, M. Y.; Smith, B. D.; Liu, J. *J. Am. Chem. Soc.* **2010**, *132*, 12668–12673.
(29) Olsen, K. G.; Ross, D. J.; Tarlov, M. J. *Anal. Chem.* **2002**, *74*, 1436–1441.
(30) Meiring, J. E.; Schmid, M. J.; Grayson, S. M.; Rathsack, B. M.; Johnson, D. M.; Kirby, R.; Kannappan, R.; Manthiram, K.; Hsia, B.; Hogan, Z. L.; et al. *Chem. Mater.* **2004**, *16*, 5574–5580.
(31) Lewis, C. L.; Choi, C.-H.; Lin, Y.; Lee, C.-S.; Yi, H. *Anal. Chem.* **2010**, *82*, 5851–5858.
(32) Pregibon, D. C.; Doyle, P. S. *Anal. Chem.* **2009**, *81*, 4873–4881.
(33) Murakami, Y.; Maeda, M. *Biomacromolecules* **2005**, *6*, 2927–2929.
(34) Um, S. H.; Lee, J. B.; Park, N.; Kwon, S. Y.; Umbach, C. C.; Luo, D. *Nat. Mater.* **2006**, *5*, 797–801.
(35) Liedl, T.; Dietz, H.; Yurke, B.; Simmel, F. *Small* **2007**, *3*, 1688–1693.
(36) Lee, C. K.; Shin, S. R.; Lee, S. H.; Jeon, J.-H.; So, I.; Kang, T. M.; Kim, S. I.; Mun, J. Y.; Han, S.-S.; Spinks, G. M.; et al. *Angew. Chem., Int. Ed.* **2008**, *47*, 2470–2474.

(37) Cheng, E. J.; Xing, Y. Z.; Chen, P.; Yang, Y.; Sun, Y. W.; Zhou, D. J.; Xu, L. J.; Fan, Q. H.; Liu, D. S. *Angew. Chem., Int. Ed.* **2009**, *48*, 7660–7663.
(38) Tang, H. W.; Duan, X. R.; Feng, X. L.; Liu, L. B.; Wang, S.; Li, Y. L.; Zhu, D. B. *Chem. Commun.* **2009**, 641–643.
(39) Venkatesh, S.; Wower, J.; Byrne, M. E. *Bioconjug. Chem.* **2009**, *20*, 1773–1782.
(40) Topuz, F.; Okay, O. *Biomacromolecules* **2009**, *10*, 2652–2661.
(41) Soontornworajit, B.; Zhou, J.; Wang, Y. *Soft Matter* **2010**, *6*, 4255–4261.
(42) Lu, Z. R.; Kopeckova, P.; Kopecek, J. *Macromol. Biosci.* **2003**, *3*, 296–300.
(43) Miyata, T.; Asami, N.; Uragami, T. *Nature* **1999**, *399*, 766–769.
(44) Miyata, T.; Asami, N.; Uragami, T. *Macromolecules* **1999**, *32*, 2082–2084.
(45) Ben-Moshe, M.; Alexeev, V. L.; Asher, S. A. *Anal. Chem.* **2006**, *78*, 5149–5157.
(46) Kim, J.; Nayak, S.; Lyon, L. A. *J. Am. Chem. Soc.* **2005**, *127*, 9588–9592.
(47) Russell, R. J.; Pishko, M. V.; Gefrides, C. C.; McShane, M. J.; Cote, G. L. *Anal. Chem.* **1999**, *71*, 3126–3132.
(48) Park, S.; Lee, Y.; Kim, D. N.; Jang, E.; Koh, W. G. *React. Funct. Polym.* **2009**, *69*, 293–299.
(49) Yan, J.; Sun, Y. H.; Zhu, H.; Marcu, L.; Revzin, A. *Biosens. Bioelectron.* **2009**, *24*, 2604–2610.
(50) Bonanno, L. M.; DeLouise, L. A. *Adv. Funct. Mater.* , *20*, 573–578.
(51) Lee, N. Y.; Jung, Y. K.; Park, H. G. *Biochem. Eng. J.* **2006**, *29*, 103–108.
(52) Hurst, S. J.; Lytton-Jean, A. K. R.; Mirkin, C. A. *Anal. Chem.* **2006**, *78*, 8313–8318.
(53) Hurst, S. J.; Hill, H. D.; Mirkin, C. A. *J. Am. Chem. Soc.* **2008**, *130*, 12192–12200.
(54) Dhar, S.; Daniel, W. L.; Giljohann, D. A.; Mirkin, C. A.; Lippard, S. J. *J. Am. Chem. Soc.* **2009**, *131*, 14652–14653.
(55) Xue, X.; Xu, W.; Wang, F.; Liu, X. *J. Am. Chem. Soc.* **2009**, *131*, 11668–11669.
(56) Liu, X. O.; Atwater, M.; Wang, J. H.; Huo, Q. *Colloid Surf. B* **2007**, *58*, 3–7.

AM100780D